



Saharan dust aerosol
over the central
Mediterranean Sea

M. Marconi et al.

This discussion paper is/has been under review for the journal Atmospheric Chemistry and Physics (ACP). Please refer to the corresponding final paper in ACP if available.

Saharan dust aerosol over the central Mediterranean Sea: optical columnar measurements vs. aerosol load, chemical composition and marker solubility at ground level

M. Marconi¹, D. M. Sferlazzo², S. Becagli¹, C. Bommarito³, G. Calzolai⁴, M. Chiari⁴, A. di Sarra⁵, C. Ghedini¹, J. L. Gómez-Amo⁵, F. Lucarelli⁴, D. Meloni⁵, F. Monteleone³, S. Nava⁴, G. Pace⁵, S. Piacentino³, F. Rugi¹, M. Severi¹, R. Traversi¹, and R. Udisti¹

¹Department of Chemistry, University of Florence, Sesto Fiorentino, Florence, 50019, Italy

²ENEA, Laboratory for Earth Observations and Analyses, 92010, Lampedusa, Italy

³ENEA, Laboratory for Earth Observations and Analyses, 90141, Palermo, Italy

⁴Department of Physics and Astronomy, University of Florence and I.N.F.N., Florence, Via Sansone 1, 50019 Sesto F.no, Florence, Italy

⁵ENEA Laboratory for Earth Observations and Analyses, 00123, Rome, Italy

Title Page

Abstract

Introduction

Conclusions

References

Tables

Figures



Back

Close

Full Screen / Esc

Printer-friendly Version

Interactive Discussion



Received: 5 June 2013 – Accepted: 30 July 2013 – Published: 14 August 2013

Correspondence to: S. Becagli (silvia.becagli@unifi.it)

Published by Copernicus Publications on behalf of the European Geosciences Union.

ACPD

13, 21259–21299, 2013

**Saharan dust aerosol
over the central
Mediterranean Sea**

M. Marconi et al.

Title Page

Abstract

Introduction

Conclusions

References

Tables

Figures



Back

Close

Full Screen / Esc

Printer-friendly Version

Interactive Discussion



Abstract

This study aims at the determination of the mineral contribution to PM_{10} in the central Mediterranean Sea on the basis of 7 yr of PM_{10} chemical composition daily measurements made on the island of Lampedusa (35.5° N, 12.6° E). Aerosol optical depth measurements are carried out in parallel while sampling with a multi-stage impactor, and observations with an optical particle counter were performed in selected periods. Based on daily samples, the total content and soluble fraction of selected metals are used to identify and characterize the dust events. The total contribution is determined by PIXE (particle-induced X-ray emission) while the composition of the soluble fraction by ICP-AES (inductively coupled plasma atomic emission spectroscopy) after extraction with HNO_3 at pH 1.5.

The average PM_{10} concentration at Lampedusa calculated over the period June 2004–December 2010 is $31.5 \mu g m^{-3}$, with low interannual variability. The annual means are below the EU annual standard for PM_{10} , but 9.9% of the total number of daily data exceed the daily threshold value established by the European Commission for PM ($50 \mu g m^{-3}$, European Community, EC/30/1999).

The Saharan dust contribution to PM_{10} was derived by calculating the contribution of Al, Si, Fe, Ti, non-sea-salt (nss) Ca, nssNa, and nssK oxides in samples in which PIXE data were available. Cases with crustal content exceeding the 75th percentile of the crustal oxide content distribution were identified as dust events. Using this threshold we identify 175 events; 31.6% of them (55 events) present PM_{10} higher than $50 \mu g m^{-3}$, with dust contributing by 33% on average.

The annual average crustal contribution to PM_{10} is $5.42 \mu g m^{-3}$, reaching a value as high as $67.9 \mu g m^{-3}$, 49% of PM_{10} , during an intense Saharan dust event. The crustal aerosol amount and contribution to PM_{10} shows a very small seasonal dependence; conversely, the dust columnar burden displays an evident annual cycle, with a strong summer maximum (monthly average aerosol optical depth at 495.7 nm up to 0.28 in June–August). We found that 71.3% of the events identified from optical properties

Saharan dust aerosol over the central Mediterranean Sea

M. Marconi et al.

Title Page

Abstract

Introduction

Conclusions

References

Tables

Figures

◀

▶

◀

▶

Back

Close

Full Screen / Esc

Printer-friendly Version

Interactive Discussion



cloud condensation nuclei (Levin et al., 1996). The investigation of the role that dust plays on climate is among the main priorities to reduce uncertainties in future climate projections (Engelstaedter et al., 2006).

Dust may also greatly increase the atmospheric levels of PM, adversely affecting air quality. This effect is especially relevant in southern and eastern Europe (Escudero et al., 2005, 2007; Pederzoli et al., 2010; Gerasopoulos et al., 2006; Dayan et al., 1991) due to the transport processes from Africa and the Arabian Peninsula and due to the relatively low precipitation, which causes a long residence time of PM in the Mediterranean atmosphere (Querol et al., 2009). Intense dust transport episodes may cause health impacts due to the high levels of PM, to which transport of anthropogenic pollutants may be associated (Erel et al., 2006).

Thus, many recent studies have focused on the estimation of the African dust influence on air quality in southern European countries, and especially in Spain and Italy (Rodriguez et al., 2001; Escudero et al., 2007; Perrino et al., 2008; Nava et al., 2012). Recent analyses by Kallos et al. (2007) and Astitha et al. (2008) have shown that, in the period 2001–2005, desert dust is present in approximately 50 % of the days with exceedances of the PM₁₀ EU limit.

In addition, dust particles frequently act as reaction surfaces for reactive gases (Den- tner et al., 1996; Levin et al., 1996), affecting atmospheric chemical processes. Dust influences atmospheric chemistry also through modulation of the solar radiation, particularly in the ultraviolet spectral range, thus influencing photochemical processes (Casasanta et al., 2011; Meloni et al., 2003). Furthermore, observations in southern Europe show that the atmospheric deposition of specific nutrients is enhanced by dust input from northern Africa (Avila and Rodà 2002). Mediterranean marine regions are highly influenced by crustal dust deposition, which may provide large amounts of nutrients for phytoplankton (Béthoux et al., 1996; Guerzoni et al., 1999). However, the processes that control the speciation and cycling of micronutrients in the surface ocean after dust deposition are scarcely known (Baker and Croot, 2010), and the hypotheses about biogeochemical responses to sporadic input of dust are controversial (Wagener

Saharan dust aerosol over the central Mediterranean Sea

M. Marconi et al.

Title Page

Abstract

Introduction

Conclusions

References

Tables

Figures

◀

▶

◀

▶

Back

Close

Full Screen / Esc

Printer-friendly Version

Interactive Discussion



et al., 2010). For this purpose, the study of the micro-nutrient solubility in aerosol is particularly useful in determining their bioavailability and to understand the biochemical processes at the ocean–atmosphere interface.

Due to the range of mechanisms in which dust is involved, the characterization of its evolution and chemical composition is very important, especially in the central Mediterranean Sea, where experimental studies are scarce. In this study we present the evolution of dust markers in aerosol samples collected on the island of Lampedusa throughout the period June 2004–December 2010. The study aims at quantifying the Saharan dust contribution to PM₁₀ at the ground level and assessing its seasonal evolution also in comparison with spectral aerosol optical depth, used as an indicator of columnar aerosol burden. Solubility of the different markers is also discussed with respect to size distribution and aerosol sources, with the objective to quantify the fraction of each analysed element able to interact with the biological system (fertilization processes by Fe or environmental toxicity by heavy metals).

2 Methods

2.1 Sampling

Chemical and physical characterization of the aerosol samples collected at remote sites is crucial to ascertain the influence of natural sources on PM. In this regard the island of Lampedusa (35.5° N, 12.6° E), which is located in the central Mediterranean Sea at least 100 km from the nearest Tunisian coast, is an ideal sampling site. The island covers a total area of about 20 km²; its soils are practically devoid of vegetation. About 6000 inhabitants live stably in Lampedusa, but during summer this number significantly grows due to its importance as a tourism destination. Industrial activities are very scarce (fish canning industry). Local aerosol sources are very low, and the main anthropic source arises from ships crossing the Mediterranean Sea about 100 km north with respect to the sampling site (Becagli et al., 2012). The aerosol sampler is posi-

Saharan dust aerosol over the central Mediterranean Sea

M. Marconi et al.

Title Page

Abstract

Introduction

Conclusions

References

Tables

Figures



Back

Close

Full Screen / Esc

Printer-friendly Version

Interactive Discussion



**Saharan dust aerosol
over the central
Mediterranean Sea**

M. Marconi et al.

Title Page

Abstract

Introduction

Conclusions

References

Tables

Figures

◀

▶

◀

▶

Back

Close

Full Screen / Esc

Printer-friendly Version

Interactive Discussion



tioned on a 45 m.a.s.l. plateau on the north-eastern coast of Lampedusa, at the Station for Climate Observations maintained by ENEA (the national Agency for New Technologies, Energy, and Sustainable Economic Development of Italy). At this site continuous observations of greenhouse gases (Artuso et al., 2009, 2010), aerosol properties (di Sarra et al., 2011; Meloni et al., 2006; Pace et al., 2006), total ozone (Gomez Amo et al., 2012), ultraviolet irradiance (di Sarra et al., 2002; Meloni et al., 2005; Arola et al., 2009; Mateos et al., 2013), surface radiation budget (di Sarra et al., 2008; Di Biagio et al., 2010) and other climatic parameters are carried out. Aerosol optical properties are measured with a multi-filter rotating shadow band radiometer (MFRSR; Harrison et al., 1994). The MFRSR is a seven-channel radiometer which measures global and diffuse irradiances, and allows the determination of column aerosol optical depth at five wavelengths (416, 496, 615, 671, and 869 nm). The measurement details and data retrieval are described by Pace et al. (2006). The aerosol PM₁₀ daily sampling is carried out by using a low volume sequential sampler (TECORA Skypost) in accordance with EN12341. The sampling campaign was started in June 2004 alternating in sequence samplings of PM₁₀, PM_{2.5}, and PM_{1.0}. Starting from 2007, only the PM₁₀ sampling was carried out on a daily basis. During the sampling period some interruptions occurred due to technical failures. The sample collection was carried out at constant flow of 2.3 m³ h⁻¹ over the time of 24 h; 47 mm diameter 2 μm pore Pall–Gelman Teflon filters were used. In order to evaluate PM₁₀ concentration (μg m⁻³), we used the gravimetric method: filters were weighted before and after sampling, and the sampling volume was provided by the sampler. Before weighing, all filters were conditioned for at least 24 h at a relative humidity of 50 % and temperature of 20 °C.

Additional 3-day resolution sampling with an Andersen 8-stage impactor working at constant flow of 1.7 m³ h⁻¹ was performed in Lampedusa in summer 2006. Each polycarbonate membrane was used to determine the ionic composition and metal content soluble at pH 1.5 and by HNO₃-H₂O₂ in microwave oven (see Sect. 2.1).

The particle size distribution was measured at the surface using a Grimm 107 optical particle counter (OPC). The Grimm was deployed at Lampedusa from 28 April to 9

June 2008 measuring the segregated size distribution in 31 diameter channels between 0.25 and 32 μm with 1 min time resolution.

2.2 Chemical analysis

A quarter of each filter (the Teflon filter from the PM_{10} daily sampling, and the polycarbonate filter from the 8-stage impactor sampling) was extracted using about 10 mL of Milli-Q water in an ultrasonic bath for 15 min, and the ionic load (Na^+ , NH_4^+ , K^+ , Mg^{2+} , Ca^{2+} , F^- , Cl^- , NO_3^- , SO_4^{2-} , methanesulfonate – MS^- , acetate, formate, glycolate, oxalate) was evaluated by 2 Dionex DX1000 and one Dionex DX500 ion chromatographs working in parallel (Becagli et al., 2011). On another quarter of filter, the analysis of selected metals was performed after extraction in an ultrasonic bath for 15 min with Milli-Q water acidified at pH 1.5–2 with ultrapure nitric acid obtained by sub-boiling distillation. In this way we derived the soluble fraction of the PM usually more available for the ecosystem. This extraction was used for the determination of 13 elements (Al, As, Ba, Cd, Cr, Cu, Fe, Mn, Mo, Ni, Pb, V, Zn) by inductively coupled plasma atomic emission spectrometer (ICP-AES, Varian 720-ES) equipped with an ultrasonic nebulizer (U5000 AT+, Cetac Technologies Inc.) by using the internal standard calibration procedure (100 ppb of Ge used as internal standard). Finally, the remaining half Teflon filters were analysed by particle-induced X-ray emission (PIXE) technique (Chiari et al., 2005; Lucarelli et al., 2011) in order to obtain the total elemental composition (soluble + insoluble). PIXE measurements were performed at the aerosol-dedicated experimental set-up (Calzolari et al., 2006) available at the LABEC laboratory of the National Institute of Nuclear Physics (INFN) in Florence, equipped with a 3 MV Tandatron accelerator. PIXE analysis was carried out on a reduced number of samples; therefore, the total elemental composition is available for a restricted data set (December 2004–December 2005, and January 2007–December 2008).

The extraction procedure in accordance with the UNI EN 14902 2005 methodology, by using HNO_3 and H_2O_2 in a microwave oven, was applied for metal determination to a quarter of the polycarbonate filters from the 8-stage impactor sampling. Actually,

Saharan dust aerosol over the central Mediterranean Sea

M. Marconi et al.

Title Page

Abstract

Introduction

Conclusions

References

Tables

Figures

◀

▶

◀

▶

Back

Close

Full Screen / Esc

Printer-friendly Version

Interactive Discussion



this procedure is not able to dissolve the silica matrix, and metals trapped in this matrix cannot be completely dissolved especially in samples with high mineral content. The efficiency of the extraction procedure was tested in PM₁₀ certified standard (NIST URBAN DUST 1649a), for Fe, Mn, Pb, Ba, and V. Recovery efficiencies were in the range of certified standards. Then the amount of the metals determined applying this extraction procedure could be near to the total content. In the used standard, Al was not certified, and the recovery efficiency of Al was determined by comparison with the total Al content measured by PIXE in PM₁₀ and PM_{2.5} urban aerosol. We found that the average recovery efficiency of Al was of 75 % (unpublished data).

3 Results and discussion

3.1 PM₁₀ concentration and contribution of crustal aerosol to PM₁₀

Figure 1 shows the daily values of PM₁₀ in the period June 2004–December 2010. The average PM₁₀ concentration over the considered period is 31.5 µg m⁻³ (average over 1134 samples). In spite of the large variability in daily values, the mean value agrees with those measured at Finokalia (35.5 µg m⁻³) and Erdemli (36.4 µg m⁻³), sites of the same typology (natural, rural) in the eastern Mediterranean region (Koçak et al., 2007, and references therein). Conversely, these values are higher than those reported by Pey et al. (2013) for rural background sites across the Mediterranean region likely due to the different elevation of the sampled sites and the different dust impact.

The PM₁₀ annual mean, even if calculated on different numbers of values, does not show a large interannual variability, ranging from 26.1 µg m⁻³ in 2005 to 33.9 µg m⁻³ in 2010. In spite of the mean annual PM₁₀ being quite high, they are below the EU annual PM₁₀ standard for PM₁₀ (40 µg m⁻³); 112 days (corresponding to 9.9% of the total number of daily data) exceed the daily threshold value established by the European Commission for PM (50 µg m⁻³, European Community, EC/30/1999). The percentage of the exceedances is higher than admitted by the EU law: 35 days yr⁻¹, corresponding

Title Page

Abstract

Introduction

Conclusions

References

Tables

Figures

◀

▶

◀

▶

Back

Close

Full Screen / Esc

Printer-friendly Version

Interactive Discussion



to 9.6%. It has to be noticed that the annual mean values and the number of exceedances have to be calculated over 90 % of the year in order to be compared with the limit imposed by the EU rules, but in our data set, although the whole year is covered by the sampling, only in the years 2007 and 2008 more than 80 % of the day in the year is sampled.

It is known that PM₁₀ concentrations are strongly influenced by the occurrence of African dust events over the Mediterranean region. In order to quantify the impact of Saharan dust intrusion episodes on PM₁₀ concentrations, the mineral content was estimated as the sum of the contributions of all the main crustal element oxides (SiO₂, Al₂O₃, Fe₂O₃, CaO, Na₂O, MgO, K₂O, TiO₂), following the approach reported in literature by several authors (Eldred et al., 1987; Malm et al., 1994; Miranda et al., 1994; Marcazzan et al., 2001; Nava et al., 2012):

$$[\text{crustal content}] = 2.14[\text{Si}] + 1.89[\text{Al}] + 1.43[\text{Fe}] + 1.40[\text{Ca}] + 1.35[\text{Na}] \\ + 1.66[\text{Mg}] + 1.21[\text{K}] + 1.67[\text{Ti}].$$

Some corrections were however applied to this formula to take into account the sea salt contributions to Na, Mg, K, and Ca, which may be relevant on Lampedusa, and possible anthropogenic contributions to the other elements.

In particular, the non-sea-salt (nss) Na⁺, nssCa²⁺, nssMg²⁺, and nssK⁺ fractions were calculated by the 5-equation system reported below:

$$\text{nssNa} = \text{nssCa} \cdot (\text{Na/Ca})_{\text{crust}}$$

$$\text{nssCa} = \text{Ca} - \text{ssCa} = \text{Ca} - \text{ssNa} \cdot (\text{Ca/Na})_{\text{seawater}}$$

$$\text{nssMg} = \text{Mg} - \text{ssMg} = \text{Mg} - \text{ssNa} \cdot (\text{Mg/Na})_{\text{seawater}}$$

$$\text{nssK} = \text{K} - \text{ssK} = \text{K} - \text{ssNa} \cdot (\text{K/Na})_{\text{seawater}}$$

where

$$\text{ssNa} = \text{Na} - \text{nssNa} = \text{Na} - \text{nssCa} \cdot (\text{Na/Ca})_{\text{crust}}$$

21268

Saharan dust aerosol over the central Mediterranean Sea

M. Marconi et al.

Title Page

Abstract

Introduction

Conclusions

References

Tables

Figures

◀

▶

◀

▶

Back

Close

Full Screen / Esc

Printer-friendly Version

Interactive Discussion



Saharan dust aerosol over the central Mediterranean Sea

M. Marconi et al.

Title Page

Abstract

Introduction

Conclusions

References

Tables

Figures

◀

▶

◀

▶

Back

Close

Full Screen / Esc

Printer-friendly Version

Interactive Discussion

and where Ca, K, and Mg represent the concentrations of these elements actually measured by PIXE in the samples. Na represents the concentration measured by ion chromatography in each sample. The concentration by ion chromatographic determination was chosen for Na because of the high error in PIXE measurements for this element.

Besides, all Na salts are water-soluble, and then the soluble fraction can be considered the total concentration. The “ss” and “nss” stand for “sea salt” and “non-sea-salt”, respectively. For $(\text{Na}/\text{Ca})_{\text{crust}}$ we used the value of 0.56, which is the mean ratio in the earth’s crust (Henderson and Henderson, 2009); for $(\text{Ca}/\text{Na})_{\text{seawater}}$, $(\text{Mg}/\text{Na})_{\text{seawater}}$, and $(\text{K}/\text{Na})_{\text{seawater}}$ the values 0.038, 0.119, and 0.037 were assumed, respectively (Henderson and Henderson, 2009), as they represent the mean ratios in bulk seawater. Ratios are expressed as weight to weight [w/w]. In the Lampedusa aerosol, the calculated mean non-sea-salt fraction for Na, Ca, Mg, and K are 11.2 %, 87.1 %, 36.9 %, and 65.6 %, respectively.

Possible anthropogenic contributions to Al, nssK, and Fe were estimated by the use of aerosol–crust enrichment factors (EFs), which were calculated with respect to Si using the upper continental crust composition in EF calculation (Henderson and Henderson, 2009). Only few samples present EF higher than 10 for Fe and about 10 % of the samples for nssK. However, since the nssK concentration is very low with respect to the other crustal markers, we used also nssK for the crustal content calculation, instead of recalculating its contribution from another oxide.

Figure 2a shows the temporal evolution of the PM_{10} mass concentration and of the crustal oxide content from January 2007 to December 2008, when continuous daily sampling and PIXE analyses were performed. Daily values and 5-day running averages correspond respectively to black and red dots and lines; only mean values of at least 3 days are shown. The percentage of crustal content on the PM_{10} value is shown in Fig. 2b, dots and lines respectively indicating daily measurements and 5-day running averages. The average crustal content is $5.42 \mu\text{g m}^{-3}$, and reaches values as high as $67.9 \mu\text{g m}^{-3}$ during intense Saharan dust events.

**Saharan dust aerosol
over the central
Mediterranean Sea**

M. Marconi et al.

Title Page

Abstract

Introduction

Conclusions

References

Tables

Figures

◀

▶

◀

▶

Back

Close

Full Screen / Esc

Printer-friendly Version

Interactive Discussion

Due to the complexity of instrumentation for the total chemical analysis and in particular for Si determination, other methods have been proposed for the quantification of Saharan dust content. In particular, Escudero et al. (2007), by using only PM_{10} measurements, estimated the daily net dust load in PM_{10} attributable to an African episode in a given region by subtracting the daily regional background level from the PM_{10} concentration. Such a method was accepted by the European Commission to establish guidelines for demonstration and subtraction of exceedances attributable to natural sources under the Directive 2008/50 EC⁻¹ on ambient air quality and cleaner air for Europe (http://ec.europa.eu/environment/air/quality/legislation/pdf/sec_2011_0208.pdf). The daily regional background level can be obtained by applying a monthly moving 40th percentile, instead of the less conservative method using 30th percentile by Escudero et al. (2007), to the PM_{10} time series at a regional background station after a prior extraction of the data of the days with African dust transport. By applying this procedure to our data set, we obtain a good correlation with crustal content calculation by oxides for Saharan dust events ($R = 0.852$, $n = 147$), but the crustal content obtained following the method from EU guidelines is 1.79 times higher than the one obtained from the sum of the metal oxides. Thus, it appears that the method proposed in the EC guidelines for the determination of the Saharan dust contribution to PM_{10} is not properly applicable to a site like Lampedusa, which is characterized by a very high contribution of background sources. Indeed, by considering the only sea-salt aerosol, it constitutes 28 % on average, and other species from other sources have to be considered for evaluation of the PM_{10} background values (sulfate, nitrate, ammonium). In this way the 40th percentile of PM_{10} represents a non-crustal background too low for this site.

Alternatively, the crustal content has been estimated from a single tracer. The most commonly used marker is Al concentration (e.g. Rodriguez et al., 2012, and references therein), considering that it represents 8.2 % of the upper continental crust (Henderson and Henderson, 2009). Comparing the crustal content obtained in this way with that

obtained as the sum of the crustal oxides, we obtain a very good correspondence between the two data sets: $R = 0.984$, $n = 698$, and slope = 1.0.

The average non-crustal PM_{10} concentration, obtained by subtracting the crustal content from the total PM_{10} concentration, is $25.7 \mu\text{g m}^{-3}$ (average over 698 samples measured during the years when PIXE data are available). Over this data set 68 PM_{10} values are higher than $50 \mu\text{g m}^{-3}$ (9.7 % of the total, similar percentage to those found for the whole data set 2004–2010), and 29 values (4.2 % of the total) of non-crustal PM_{10} exceeded the threshold. In order to understand the causes of such exceedances, it has to be considered that sea spray is the second most important aerosol source on Lampedusa island. In the considered data set, sea spray accounts on average for $8.6 \mu\text{g m}^{-3}$ (28 % of the PM_{10}) and for $18.7 \mu\text{g m}^{-3}$ on days when the non-crustal PM_{10} is higher than $50 \mu\text{g m}^{-3}$.

A criterion based on the crustal content was defined with the aim of identifying Saharan dust events. Cases with crustal content exceeding the 75th percentile of the crustal oxide content distribution (corresponding to $5.44 \mu\text{g m}^{-3}$) were identified as dust events. Using this threshold we identify 174 samples characterized by a strong crustal contribution; on average, for these samples dust constitutes 34 % of the PM_{10} . However, since PIXE analyses are available over limited time intervals, a different criterion applicable to the whole data set was defined to identify Saharan dust events; this criterion is based on the amount of nssCa measured with ion chromatography. We classify as dust events all cases with nssCa exceeding the 75th percentile of the nssCa distribution (483 ng m^{-3}). Although nssCa is only one of the elements used for the determination of the crustal content, and the Ca determined by ion chromatography is about 75 % of the total Ca during Saharan dust events (see Sect. 3.4), it displays a good correlation with the crustal content ($R = 0.869$, $n = 698$, $p < 0.01$) and proves to be a reliable marker of Saharan dust events. The selection based on this threshold on nssCa results to be slightly more restrictive than the one based on the total crustal content. Indeed, by using the two criteria when both measurements are performed, we found that the samples which exceed the nssCa concentration threshold are 85 % of those found on

Saharan dust aerosol over the central Mediterranean Sea

M. Marconi et al.

Title Page

Abstract

Introduction

Conclusions

References

Tables

Figures

◀

▶

◀

▶

Back

Close

Full Screen / Esc

Printer-friendly Version

Interactive Discussion



the basis of the total crustal content. Anyway, back-trajectory analysis shows that all the selected events by nssCa are characterized by air masses at almost one altitude (500, 1000 or 3000 m.a.s.l.) arising from Sahara desert.

Measurements of crustal oxide content, PM₁₀ mass concentration and the values of their ratio when nssCa > 483 ngm⁻³ are shown in Fig. 2 by yellow, cyan and black open squares respectively.

By comparison, we use other identification methods based on ground-based measurements of column aerosol optical properties (Meloni et al., 2008) and air mass back-trajectory analysis (Pace et al., 2006; Pederzoli et al., 2010).

A characterization of the aerosol types present over the atmospheric column can be based on measurements of the aerosol optical depth at 495.7 nm (τ) and Ångström exponent (α) calculated from the aerosol optical depth at 415.6 nm and 868.7 nm. While τ is directly proportional to the aerosol column density (number of particles), α mainly depends on the particle size distribution (low values of α indicate a prevailing role of coarse particles). The combined use of τ and α allows the identification of different aerosol types, including dust: usually, high values of τ associated with low values of α are typical of Saharan dust (Pace et al., 2006).

Figure 3 shows the behaviour of average values of α vs. τ for cloud-free conditions for those days in which ionic composition measurements are available in the time period between June 2004 and December 2010. The average values are calculated for the duration of each daily sampling. A total of 776 values are used. Red markers identify the 193 (i.e. 24.9% of the total) days with large dust amount selected on the basis of the nssCa content (i.e. nssCa²⁺ > 483 μgm^{-3}). As suggested by Pace et al. (2006), the combined thresholds of $\tau > 0.15$ and $\alpha < 0.5$ are used to identify Saharan dust events from the column optical properties. We found that 71.3% (129 episodes) of the events identified using the optical properties (181, i.e. 23.3% of the total) display a high nssCa, while 28.7% of the dust events selected by α and τ present low concentrations of nssCa. A plausible reason for these results is that Saharan dust transport frequently

Saharan dust aerosol over the central Mediterranean Sea

M. Marconi et al.

Title Page

Abstract

Introduction

Conclusions

References

Tables

Figures

◀

▶

◀

▶

Back

Close

Full Screen / Esc

Printer-friendly Version

Interactive Discussion



intense columnar episodes, they do not increase the occurrence of a simultaneous event at surface, indicating that the columnar amount of dust does not play the main role in determining the presence of dust at surface in these seasons.

In summer, surface episodes present almost the same frequency of occurrence with (45.6 %) or without (54.4 %) simultaneous columnar episodes. These results change if cases of intense surface episodes are considered, presenting a 70 % frequency that the event takes place during a columnar episode.

This suggests that when large amounts of dust are present on the column, the penetration in the marine boundary layer may be favoured, especially for long-lasting episodes.

Differently from the other seasons, in summer columnar events do not necessarily correspond to surface events, the frequency being 55.9 %, and the correspondence further decreases when intense columnar episodes are taken into account.

In summer the presence of dust at surface and on the whole column shows the minimum correspondence, supporting the idea that the strength of the summer convection over the Sahara injects desert dust at high altitudes and that particles, advected over the stable marine boundary layer, seldom influence the surface aerosol amount.

3.2 Seasonality of PM_{10} and Saharan dust events

Figure 4 shows the monthly distribution of PM_{10} , nssCa, and τ for the period June 2004–December 2010. The aerosol optical depth shows a marked seasonal pattern with spring–summer maxima. Previous studies reported that the dust optical depth and vertical distribution show a large seasonal cycle, with elevated τ and a wider vertical extension in spring and summer; the seasonal change is mainly controlled by dust transport occurring over the boundary layer (Di Iorio et al., 2009). On the contrary, PM_{10} and nssCa show no evident seasonal pattern, both in median values and in variability, which is however lower during summertime. PM_{10} appears marginally higher during spring. Since τ provides information on the entire air column, high values of τ in spring and summer do not necessarily imply that a high aerosol load is present close

Saharan dust aerosol over the central Mediterranean Sea

M. Marconi et al.

Title Page

Abstract

Introduction

Conclusions

References

Tables

Figures

◀

▶

◀

▶

Back

Close

Full Screen / Esc

Printer-friendly Version

Interactive Discussion



to the surface, where PM_{10} and nssCa are measured. Nevertheless, peaks in the 95th percentile occur in the same months for both PM_{10} and nssCa, confirming that very high PM_{10} values are associated with dust, when the marine boundary layer shows a weaker separation from the upper atmosphere.

Figure 5 reports the percentage of days of Saharan dust events occurring in each month as estimated from the column optical properties and from the threshold on nssCa, and the number of days with $PM_{10} > 50 \mu g m^{-3}$ expressed in percent. The figure shows a very different annual pattern of the percentage of Saharan dust days identified from chemical and optical properties. The seasonal pattern of Saharan dust events identified by optical properties shows a well-defined summer maximum, as also reported by several authors over the central Mediterranean region; conversely, the Saharan dust days at the ground level show a very different pattern, with a high occurrence of events in March–April and October–November and minimum occurrence in summer. Besides, the intensity of Saharan dust surface events in February, April and October–November are more intense than those of other months. The mean percentage of events at ground level and their intensity pattern agree with results found by Pey et al. (2013) for the central Mediterranean Sea. Conversely, the minimum in percentage of Saharan dust event in summer was not detected by Pey et al. (2013) in the analysed site in central Mediterranean. Besides, the difference between the results of the two methods (optical and chemical) is maximum in summer. This evidence suggests that in summer air masses coming from Saharan desert overpass the boundary layer over this area, and no significant mixing between inside and above the boundary layer occurs. A previous study showed that in summer African dust episodes over the western and central part of the Mediterranean basin have lower intensity than other seasons and occur at high altitude. This is due to the presence of the Atlas Mountain barrier (2500 km extension and peak altitudes up to more than 4000 m a.s.l.) that plays a dominant role in local and mesoscale atmospheric circulation patterns (Pey et al., 2013). Besides, higher stability of the marine boundary layer in summer than in the

Saharan dust aerosol over the central Mediterranean Sea

M. Marconi et al.

Title Page

Abstract

Introduction

Conclusions

References

Tables

Figures

◀

▶

◀

▶

Back

Close

Full Screen / Esc

Printer-friendly Version

Interactive Discussion



other seasons over the Mediterranean Sea (Dayan et al., 1989) prevents the mixing between low and high atmospheric layers.

In spring and autumn the occurrence of Saharan dust days at the ground level is higher than those over the column. As discussed previously, this is related to seasonal changes in the convection intensity over the Sahara. This situation is typical of Saharan dust events determined by transport processes affecting the eastern part of Mediterranean basin in spring and autumn. They are induced by cyclones moving eastwards across the Mediterranean and/or north Africa, transporting dust at surface levels (Pey et al., 2013).

The percentage of PM_{10} exceedances shows two maxima, in May and November; only the latter corresponds to a higher occurrence of Saharan dust events as revealed by nssCa. Other sources have to be considered to explain the high percentage of exceedances in May.

3.3 Size distribution and solubility of Saharan dust aerosol marker

The deposition of atmospheric particles to surface waters may provide nutrients to marine biological systems, and affect the marine productivity (Duce et al., 1991, Gallisai et al., 2012). These processes may be particularly relevant for oligotrophic oceans and for semi-enclosed seas, such as the Mediterranean. Most of the deposition in the Mediterranean is associated with Saharan dust events. Bioavailability of nutrients depends on several factors, and in particular on the size distribution of the deposited particles and on the solubility of the various elements. Thus, the determination of the size distribution of the different elements and their solubility is crucial to understand the potential impact of dust events on biogeochemical processes.

The solubility of several elements in HNO_3 pH 1.5 was calculated for PM_{10} samples corresponding to Saharan dust and non-Saharan dust events. Median, mean, and standard deviations of the percent solubility are reported in Table 2.

The solubility of each element presents a large variability. The solubility is in general affected by various processes, such as chemical speciation, mixing of different types of

Saharan dust aerosol over the central Mediterranean Sea

M. Marconi et al.

Title Page

Abstract

Introduction

Conclusions

References

Tables

Figures



Back

Close

Full Screen / Esc

Printer-friendly Version

Interactive Discussion



**Saharan dust aerosol
over the central
Mediterranean Sea**

M. Marconi et al.

Title Page

Abstract

Introduction

Conclusions

References

Tables

Figures

◀

▶

◀

▶

Back

Close

Full Screen / Esc

Printer-friendly Version

Interactive Discussion

particles, size distribution, and aging processes. The large variability of the measured solubility is attributed to the influence of these processes. In spite of this large variability, usually the solubility is lower in Saharan dust samples than in non-Saharan dust events, because, in the used extraction condition, only free metals, carbonates, oxide hydrates, or complexes of the elements with organic compounds are solubilized. Conversely, elements present as oxides or taking part in the silica matrices (i.e. the 66.6 % main constituent of the upper continental crust) are not solubilized with this extraction condition.

Metals emitted by anthropic sources are usually in more soluble form because of the chemical speciation and their occurrence in the finest particle fraction. Becagli et al. (2012) reported solubility of about 80 and 70 % respectively for V and Ni from heavy oil combustion sources. These values are slightly higher than those reported in Table 2 for non-Saharan dust events; the cases included in Table 2 are relative to all samples characterized by low crustal content, and not only those directly influenced by heavy oil combustion (as it was the case for Becagli et al., 2012). The V and Ni solubility are however consistent with their solubility in the finest fraction of multistage impactors (Fig. 6). Besides, the high concentration and solubility, up to 96 % for V measured in the aerosol finest fraction of multistage impactors (Fig. 6), demonstrate the presence of the anthropic source also in events characterized by high Saharan dust content.

The size distribution of various elements was determined from multi-stage impactor samples. Data from three days integrated sample characterized by high Saharan dust content (23, 24, and 25 June 2006) are reported in Fig. 6. The sampled event represents a large columnar episode ($\tau = 0.39$ and $\alpha = -0.05 \pm 0.09$) with high aerosol load and nssCa at the surface ($PM_{10} = 57.4 \mu\text{g m}^{-3}$ and $\text{nssCa} = 2050 \text{ ng m}^{-3}$ measured 23 June 2006). The concentration of each marker for each impactor stage is obtained using different extraction procedures applied on different portions of the filter: $\text{HNO}_3 + \text{H}_2\text{O}_2$ in microwave oven and HNO_3 pH 1.5 were used for all the elements; in addition, extraction in ultrapure water was also used for Mg, Ca, and K. The three

different extractions give information on the bioavailability of each elements also as a function of the size of the particle in which they are present.

Figure 6 shows that not only the typical crustal markers (Si, Al, Fe, Ca, Ti, Mn) but also elements having others sources (Mg, K, Ba) or present as trace in the crust (Li, Sc) present two relative maxima in the concentration, respectively in the size ranges 2.1–3.3 μm and 5.8–9 μm . Others trace elements taking part in the mineral matrix (Sr, Rb, La, Y, Yb, Co) present only one large maximum in the range 2.1–5.8 μm . In the examined event all the elements excluding Ca, Mg, Ba, Mn, Sr present in these coarse modes solubility lower than 15 %.

The two maxima (2.1–3.3 μm and 5.8–9 μm) agree with the aerosol size distribution obtained from OPC data for Saharan dust events. In particular, during the OPC measuring campaign in late spring 2008, all the days with significant dust contribution were identified by applying the two criteria: (a) the concentration of nssCa $> 483 \text{ ng m}^{-3}$ and (b) $\tau > 0.15$ and $\alpha < 0.5$. Four days satisfying the first criterion were used to derive the aerosol size distribution. In three out of the four days also the criterion based on the column optical properties was satisfied. The size distributions of the four days with nssCa $> 483 \text{ ng m}^{-3}$ were averaged; a fitting procedure was implemented to obtain the modal parameters assuming that the particles are distributed as a multimode lognormal function. Three different lognormal modes were identified, and their parameters are listed in Table 3.

More than 99 % of particles are in the finest mode with a median diameter at 0.29 μm . A small fraction of the particles (0.12 % of the total particles concentration) are larger than 1 μm . Conversely, the largest contribution to the total volume comes from the second mode (49.1 %) as shown in Table 3.

The finest mode is related to an anthropic source mixed with a crustal one. In fact, elements having only anthropic source or both (Fe, K, Co, Pb, V, Ni, Cd) present a maximum in the finest fraction, which is characterized by relatively high solubility. For instance, Fe present in the coarse fraction displays a very low solubility (8 % in the size range 2.1–3.3 μm). A maximum of Fe concentration in the finest particles fraction ap-

Saharan dust aerosol over the central Mediterranean Sea

M. Marconi et al.

Title Page

Abstract

Introduction

Conclusions

References

Tables

Figures

◀

▶

◀

▶

Back

Close

Full Screen / Esc

Printer-friendly Version

Interactive Discussion



**Saharan dust aerosol
over the central
Mediterranean Sea**

M. Marconi et al.

Title Page

Abstract

Introduction

Conclusions

References

Tables

Figures

◀

▶

◀

▶

Back

Close

Full Screen / Esc

Printer-friendly Version

Interactive Discussion



pears only when the soluble fraction is considered (Fig. 6), as a result of a strong increase of solubility (69% in the size range 0.4–0.7 μm) for decreasing size. It is known that the solubilization is faster and more efficient for decreasing particle size because of the increase in the available particles surface area for the same volume. Considering spherical particles, the surface-to-volume ratio increases by a factor of about 5 passing from particles in the range 2.1–3.3 μm to 0.4–0.7 μm . Consequently, the increase of solubility due to size between the two size ranges is expected to be of the order of 5. The ratio of the solubility in the two size ranges is larger than 5, suggesting that the increased solubility in the finest fraction is also due to a different speciation of Fe as a function of size.

A high solubility in the finest particles size is typical of most elements, except Si, Ti, Al, La, Y, Yb, Sc, and Rb.

The solubility of various crustal markers (Si, Al, Fe, Ti, Li, La, Y, Sc, Rb, and Co) in the 1–5 micron range is generally low, because they are present mainly as oxides or as silicates, which are not soluble in HNO_3 pH 1.5. On the other hand Ca, Mg, K, Ba, Mn, and Sr present a higher solubility in the same size range, suggesting that part of these elements are present as chloride, nitrate, sulfates and carbonates in crustal aerosols. The presence of carbonate can be estimated for Ca and Mg from the difference between the solubility in HNO_3 pH 1.5 (red line in Fig. 6) and in H_2O (blue line in Fig. 6). Indeed, Ca and Mg sulfate, chloride, and nitrate salts are soluble in H_2O ; conversely, carbonates are soluble in acid condition (HNO_3 pH 1.5). In this event the fraction of Ca and Mg present as carbonates are 20% and 18% respectively in the 1–10 micron size range.

Figure 7 shows the ionic balance calculated for each of the 7 stages of the impactor on the water extract: anions and cations are summed separately in each stage. It can be noticed that nitrate, which is mainly due to the oxidation of anthropic NO_x (then expected to appear in the finest fraction), is mainly present in particles larger than 1 micron, similar to the main crustal marker (Ca). It is known that HNO_3 formed in the gas phase in the atmosphere undergoes exchange reactions with NaCl from sea

spray, or with CaCO_3 from crustal aerosols (e.g. Fairlie et al., 2010, and references therein). The impactor data suggest that the exchange reactions with CaCO_3 constitute an important process in Saharan dust samples mixed with anthropic aerosols. This process may lead to an increase in the solubility of CaCO_3 and other carbonates.

The solubility of Ca, Mg, Fe, and Al is plotted vs. the sum of NO_3^- and SO_4^{2-} content in Fig. 8. The sum of NO_3^- and SO_4^{2-} is used to give an indication of the anthropic acidic species capable of dissolving carbonate when they are absorbed over crustal particles. Sulfate is mainly present in the finest fraction of aerosol, but its concentration in the size range of crustal markers is not negligible (red area in the ionic balances in Fig. 7), and then it can contribute, together with NO_3^- , to dissolving carbonate. Although several other factors may play a role (for instance the time of contact between the air masses enriched in anthropic acidic species and those of crustal origin), an increase of anthropic acidic species should produce an enhancement of solubility. In fact, in spite of the uncertainties and the large variability, an increase in solubility appears to be associated with elevated amounts of nitrate and sulfate, better evident for Ca and Mg. Thus, aging processes and mixing of crustal and anthropic aerosols during transport from source areas to the sampling site are able to change the aerosol chemical properties, and may affect solubility and, in turn, the bioavailability of crustal elements.

4 Conclusions

Daily PM_{10} samples collected at Lampedusa from 2004 to 2010 were analysed for total content and soluble fraction of selected elements and metals to determine the mineral contribution to PM_{10} , size distribution and solubility in the central Mediterranean Sea. From these data the following conclusion can be drawn.

In spite of the distance from aerosol pollution sources, 10 % of the total data number exceeded the daily threshold value ($50 \mu\text{g m}^{-3}$, European Community, EC/30/1999) established by the European Commission for PM (35 days/year, corresponding to 9.6 %).

Saharan dust aerosol over the central Mediterranean Sea

M. Marconi et al.

Title Page

Abstract

Introduction

Conclusions

References

Tables

Figures

◀

▶

◀

▶

Back

Close

Full Screen / Esc

Printer-friendly Version

Interactive Discussion



Saharan dust content was evaluated by main oxides (Al, Si, Fe, Ti and non-sea-salt Ca, Na, Mg, K) for samples for which a PIXE analysis was performed. On average it accounts for $5.42 \mu\text{g m}^{-3}$, but during a strong Saharan dust event it reaches the value of $67.9 \mu\text{g m}^{-3}$.

Regarding the seasonal pattern of Saharan dust events, while the column burden of desert dust displays an evident annual cycle, with a strong summer maximum, the crustal aerosol amount, contribution to PM_{10} and percentage of Saharan dust events do not show any seasonal pattern. We found that 71.3% of the events identified using the optical properties (i.e. 23.3% of the total) display high dust content at ground level, demonstrating that Saharan dust transport frequently occurs above the marine boundary layer, and no significant mixing between inside and above the boundary layer occurs. This is especially true in summer when, due to the generally higher stability of marine boundary layer, the greatest difference between percentage of Saharan dust events from optical properties and chemical markers is observed.

The size distribution of Saharan dust is achieved by optical particle counter measurements during days with high mineral content; an optimized fitting procedure is applied to obtain the modal parameters assuming that the particles are distributed as a multi-mode lognormal function. Three different lognormal modes were identified at $7.18 \mu\text{m}$, $2.23 \mu\text{m}$ and $0.293 \mu\text{m}$ median diameters. A small fraction of the particles (0.12% of the total particles concentration) are larger than $1 \mu\text{m}$. Conversely, the largest contribution to the total volume (49.1%) comes from the $2.23 \mu\text{m}$ mode.

The crustal markers present two relative maxima in the size range $5.8\text{--}9 \mu\text{m}$ and $2.1\text{--}3.3 \mu\text{m}$ accordingly with particulate size distribution; both these modes present low solubility of the element (e.g. 40% and 8% for V and Fe respectively). The third mode in the finest fraction is only present for metals having anthropic sources other than crustal sources (K, Fe, V, Ni, Co, Pb, Cd). This fraction is also characterized by higher solubility of the metal (e.g. 96% and 69% for V and Fe respectively) due both to the size of particles and the source of the metal which is present.

Saharan dust aerosol over the central Mediterranean Sea

M. Marconi et al.

[Title Page](#)[Abstract](#)[Introduction](#)[Conclusions](#)[References](#)[Tables](#)[Figures](#)[◀](#)[▶](#)[◀](#)[▶](#)[Back](#)[Close](#)[Full Screen / Esc](#)[Printer-friendly Version](#)[Interactive Discussion](#)

**Saharan dust aerosol
over the central
Mediterranean Sea**

M. Marconi et al.

Title Page

Abstract

Introduction

Conclusions

References

Tables

Figures

◀

▶

◀

▶

Back

Close

Full Screen / Esc

Printer-friendly Version

Interactive Discussion



In general, solubility of each element presents a large variability in the condition of extraction; usually in Saharan dust events the solubility is lower than in non-Saharan dust events. Besides, solubility depends on the aging processes and mixing of crustal and anthropic aerosols. Here we found that the percentage of solubility of Ca, Mg and, to a less extent, Fe and Al increases as a function of the sum of NO_3^- and SO_4^{2-} content (arising from anthropic acidic species). This is interpreted as the capacity of the mixing process to change the chemical properties of particulate matter especially on its surface, not only affecting bioavailability of elements but also increasing the capability of a particulate to form cloud condensation nuclei due to the increased affinity of aerosol with water. The study of these processes is particularly important.

Acknowledgements. The study has been partially supported by the Italian Ministry for University and Research through the SNUMMASS, NextData, and Ritmare projects.

References

- Arola, A., Kazadzis, S., Lindfors, A., Krotkov, N., Kujanpää, J., Tamminen, J., Bais, A., di Sarra, A., Villaplana, J. M., Brogniez, C., Siani, A. M., Janouch, M., Weihs, P., Koskela, T., Kouremeti, N., Meloni, D., Buchard, V., Auriol, F., Ialongo, I., Staneck, M., Simic, S., Webb, A., Smedley, A., and Kinne, S.: A new approach to correct for absorbing aerosols in OMI UV, *Geophys. Res. Lett.*, 36, L22805, doi:10.1029/2009GL041137, 2009.
- Artuso, F., Chamard, P., Piacentino, S., Sferlazzo, D. M., De Silvestri, L., di Sarra, A., Meloni, D., and Monteleone, F.: Influence of transport and trends in atmospheric CO_2 at Lampedusa, *Atmos. Environ.*, 43, 3044–3051, 2009.
- Artuso, F., Chamard, P., Chiavarini, S., di Sarra, A., Meloni, D., Piacentino, S., and Sferlazzo, D. M.: Tropospheric halocarbons and nitrous oxide monitored at a remote site in the Mediterranean, *Atmos. Environ.*, 44, 4944–4953, 2010.
- Astitha, M., Kallos, G., and Katsafados, P.: Air pollution modeling in the Mediterranean Region: analysis and forecasting of episodes, *Atmos. Res.*, 89, 358–364, 2008.
- Avila, A. and Rodà, F.: Assessing decadal changes in rainwater alkalinity at a rural Mediterranean site in the Montseny mountains (NE Spain), *Atmos. Environ.*, 36, 2881–2890, 2002.

**Saharan dust aerosol
over the central
Mediterranean Sea**

M. Marconi et al.

Title Page

Abstract

Introduction

Conclusions

References

Tables

Figures

◀

▶

◀

▶

Back

Close

Full Screen / Esc

Printer-friendly Version

Interactive Discussion



- Baker, A. R. and Croot, P. L.: Atmospheric and marine controls on aerosol iron solubility in seawater, *Mar. Chem.*, 120, 4–13, doi:10.1016/j.marchem.2008.09.003, 2010.
- Becagli, S., Ghedini, C., Peeters, S., Rottiers, A., Traversi, R., Udisti, R., Chiari, M., Jalba, A., Despiou, S., Dayan, U., and Temara, A.: MBAS (Methylene Blue Active Substances) and LAS (Linear Alkylbenzene Sulphonates) in Mediterranean coastal aerosols: sources and transport processes, *Atmos. Environ.*, 45, 6788–6801, 2011.
- Becagli, S., Sferlazzo, D. M., Pace, G., di Sarra, A., Bommarito, C., Calzolari, G., Ghedini, C., Lucarelli, F., Meloni, D., Monteleone, F., Severi, M., Traversi, R., and Udisti, R.: Evidence for heavy fuel oil combustion aerosols from chemical analyses at the island of Lampedusa: a possible large role of ships emissions in the Mediterranean, *Atmos. Chem. Phys.*, 12, 3479–3492, doi:10.5194/acp-12-3479-2012, 2012.
- Bethoux, J. P. and Gentili, B.: The Mediterranean Sea, coastal and deep-sea signatures of climatic and environmental changes, *J. Marine Syst.*, 7, 383–394, 1996.
- Bethoux, J. P., Gentili, B., Morin, P., Nicolas, E., Pierre, C., and Ruiz-Pino, D.: The Mediterranean Sea: a miniature ocean for climatic and environmental studies and a key for the climatic functioning of the North Atlantic, *Prog. Oceanogr.*, 44, 131–146, 1999.
- Bethoux, J. P., Morin, P., and Ruiz-Pino, D. P.: Temporal trends in nutrient ratios: chemical evidence of Mediterranean ecosystem changes driven by human activity, *Deep-Sea Res. II*, 49, 2007–2015, 2002.
- Calzolari, G., Chiari, M., García Orellana, I., Lucarelli, F., Migliori, A., Nava, S., and Taccetti, F.: The new external beam facility for environmental studies at the Tandatron accelerator of LABEC, *Nucl. Instr. Meth. B*, 249, 928–931, 2006.
- Casasanta, G., di Sarra, A., Meloni, D., Monteleone, F., Pace, G., Piacentino, S., and Sferlazzo, D.: Large aerosol effects on ozone photolysis in the Mediterranean, *Atmos. Environ.*, 45, 3937–3943, 2011.
- d’Almeida, G. A.: A Model for Saharan dust transport, *J. Climate Appl. Meteor.*, 25, 903–916, 1986.
- Dayan, U., Heffter, J. L., and Miller, J. M.: Meteorological and Climatological Data from Surface and Upper Measurements for the Assessment of Atmospheric Transport and Deposition of Pollutants in the Mediterranean Basin: Part B: Seasonal Distribution of the Planetary Boundary Layer Depths over the Mediterranean Basin, UNEP, Mediterranean Action Plan Technical Reports Series no. 30, Athens, Greece, 1989.

Saharan dust aerosol over the central Mediterranean Sea

M. Marconi et al.

Title Page

Abstract

Introduction

Conclusions

References

Tables

Figures

◀

▶

◀

▶

Back

Close

Full Screen / Esc

Printer-friendly Version

Interactive Discussion



- Dayan, U., Heffter, J., Miller, J., and Gutman, G.: Dust intrusion events into the Mediterranean Basin. *J. Appl. Meteorol.*, 30, 1185–1199, 1991.
- Dentener, F. J., Carmichael, G. R., Zhang, Y., Leleieveld, J., and Crutzen, P. J.: Role of mineral aerosols as a reactive surface in the global troposphere. *J. Geophys. Res.*, 101, 22869–22889, 1996.
- 5 Di Biagio, C., di Sarra, A., and Meloni, D.: Large atmospheric shortwave radiative forcing by Mediterranean aerosol derived from simultaneous ground-based and spaceborne observations, and dependence on the aerosol type and single scattering albedo, *J. Geophys. Res.*, 115, D10209, doi:10.1029/2009JD012697, 2010.
- 10 di Sarra, A., Cacciani, M., Chamard, P., Cornwall, C., DeLuisi, J. J., Di Iorio, T., Disterhoft, P., Fiocco, G., Fu'a, D., and Monteleone, F.: Effects of desert dust and ozone on the ultraviolet irradiance at the Mediterranean island of Lampedusa during PAUR II, *J. Geophys. Res.*, 107, 8135, doi:10.1029/2000JD000139, 2002.
- di Sarra, A., Pace, G., Meloni, D., De Silvestri, L., Piacentino, S., and Monteleone, F.: Surface shortwave radiative forcing of different aerosol types in the central Mediterranean, *Geophys. Res. Lett.*, 35, L02714, doi:10.1029/2007GL032395, 2008.
- di Sarra, A., Di Biagio, C., Meloni, D., Monteleone, F., Pace, G., Pugnaghi, S., and Sferlazzo, D.: Shortwave and longwave radiative effects of the intense Saharan dust event of 25–26 March 2010 at Lampedusa (Mediterranean sea), *J. Geophys. Res.*, 116, D23209, doi:10.1029/2011JD016238, 2011.
- 20 Duce, R. A., Liss, P. S., Merrill, J. T., Buat-Menard, P., Hicks, B. B., Miller, J. M., Prospero, J. M., Arimoto, R., Church, T. M., Ellis, W., Galloway, J. N., Hanson, K., Jickells, T. D., Knapp, A. H., Rienhart, K. H., Schneider, B., Soudine, A., Tokos, J. J., Tsunogai, S., Wollast, R., and Zhou, M.: The atmospheric input of trace species to the world ocean, *Global Biogeochem. Cy.*, 5, 193–259, 1991.
- 25 Eldred, R. A., Cahill, T. A., and Feeney, P. J.: Particulate monitoring at US National Parks using PIXE, *Nucl. Inst. Meth. Phys. Res. B*, 22, 289–295, 1987.
- Engelstaedter, S., Tegen, I., and Washington, R.: North African dust emissions and transport, *Earth Sci. Rev.*, 79, 73–100, 2006.
- 30 Erel, Y., Dayan, U., Rabi, R., Rudich, Y., and Stein, M.: Trans boundary transport of pollutants by atmospheric mineral dust, *Environ. Sci. Tech.*, 40, 2996–3005, 2006.

**Saharan dust aerosol
over the central
Mediterranean Sea**

M. Marconi et al.

Title Page

Abstract

Introduction

Conclusions

References

Tables

Figures

◀

▶

◀

▶

Back

Close

Full Screen / Esc

Printer-friendly Version

Interactive Discussion



Escudero, M., Castillo, S., Querol, X., Avila, A., Alarco'n, M., Viana, M. M., Alastuey, A., Cuevas, E., and Rodríguez, S.: Wet and dry African dust episodes over eastern Spain. *J. Geophys. Res.*, 110, D18S08, doi:10.1029/2004JD004731, 2005.

Escudero, M., Querol, X., Avila, A., and Cuevas, E.: Origin of the exceedances of the European daily PM limit value in the regional background areas of Spain, *Atmos. Environ.*, 41, 730–744, 2007.

Fairlie, T. D., Jacob, D. J., Dibb, J. E., Alexander, B., Avery, M. A., van Donkelaar, A., and Zhang, L.: Impact of mineral dust on nitrate, sulfate, and ozone in transpacific Asian pollution plumes, *Atmos. Chem. Phys.*, 10, 3999–4012, doi:10.5194/acp-10-3999-2010, 2010.

Gallissai, R., Peters, F., Basart, S., and Baldasano, J. M.: Mediterranean basin-wide correlations between Saharan dust deposition and ocean chlorophyll concentration, *Biogeosciences Discuss.*, 9, 8611–8639, doi:10.5194/bgd-9-8611-2012, 2012.

Gerasopoulos, E., Kouvarakis, G., Babasakalis, P., Vrekoussis, M., Putaud, J.-P., and Mihalopoulos, N.: Origin and variability of particulate matter (PM₁₀) mass concentrations over the eastern Mediterranean. *Atmos. Environ.*, 40, 4679–4690, 2006.

Gómez-Amo, J. L., Estellés, V., di Sarra, A., Pedrós, R., Utrillas, M. P., Martínez-Lozano, J. A., González-Frias, C., Kyrö, E., and Vilaplana, J. M.: Operational considerations to improve total ozone measurements with a Microtops II ozone monitor, *Atmos. Meas. Tech.*, 5, 759–769, doi:10.5194/amt-5-759-2012, 2012.

Guerzoni, S., Chester, R., Dulac, F., Herut, B., Loye-Pilot, M.-D., Measures, C., Mignon, C., Molinaroli, E., Moulin, C., Rossini, P., Saydam, C., Soudine, A., and Ziveri, P.: The role of atmospheric deposition in the biogeochemistry of the Mediterranean Sea, *Prog. Oceanogr.*, 44, 147–190, 1999.

Harrison, L., Michalsky, J., and Berndt, J.: Automated multifilter rotating shadowband radiometer: an instrument for optical depth and radiation measurements, *Appl. Optics*, 33, 5118–5125, 1994.

Henderson, P. and Henderson, G. M.: *The Cambridge Handbook of Earth Science Data*, Cambridge University Press, Cambridge, 42–44, 2009.

IPCC: *Climate Change 2007: the Physical Science Basis*, Contribution of Working Group I to the Fourth Assessment Report of the IPCC, 2007.

Kallos, G., Astitha, M., Katsafados, P., and Spyrou, C.: Long-range transport of anthropogenic and naturally produced particulate matter in the Mediterranean and north Atlantic: cur-

Saharan dust aerosol over the central Mediterranean Sea

M. Marconi et al.

Title Page

Abstract

Introduction

Conclusions

References

Tables

Figures

◀

▶

◀

▶

Back

Close

Full Screen / Esc

Printer-friendly Version

Interactive Discussion

rent state of knowledge, *J. Appl. Meteorol. Clim.*, 46, 1230–1251, doi:10.1175/JAM2530.1, 2007.

Koçak, M., Mihalopoulos, N., and Kubilay, N.: Contributions of natural sources to high PM₁₀ and PM_{2.5} events in the eastern Mediterranean, *Atmos. Environ.*, 41, 3806–3818, 2007.

5 Kouvarakis, G., Tsigaridis, K., Kanakidou, M., and Mihalopoulos, N.: Temporal variations of surface regional background ozone over Crete Island in southeast Mediterranean, *J. Geophys. Res.*, 105, 4399–4407, 2000.

Lelieveld, J. and Dentener, F. J.: What controls tropospheric ozone?, *J. Geophys. Res.*, 105, 3531–3551, 2000.

10 Levin, Z., Ganor, E., and Gladstein, V.: The effects of desert particles coated with sulfate on rain formation in the Eastern Mediterranean. *J. Appl. Meteorol.*, 35, 1511–1523, 1996.

Lucarelli, F., Nava, S., Calzolari, G., Chiari, M., Udisti, R., and Marino, F.: Is PIXE still a useful technique for the analysis of atmospheric aerosols?, The LABEC experience, *X-Ray Spectrometry*, 40, 162–167, doi:10.1002/xrs.1312, 2011.

15 Malm, W. C., Sisler, J. F., Huffman, D., Eldred, R. A., and Cahill, T. A.: Spatial and seasonal trends in particle concentration and optical extinction in the United States, *J. Geophys. Res.*, 99, 1347–1370, 1994.

Marcazzan, G. M., Vaccaro, S., Valli, G., and Vecchi, R.: Characterisation of PM₁₀ and PM_{2.5} particulate matter in the ambient air of Milan (Italy), *Atmos. Environ.*, 35, 4639–4650, 2001.

20 Marticorena, B., Bergametti, G., Aumont, B., Callot, Y., N'Doumé C., and Legrand, M.: Modelling the atmospheric dust cycle: 2-Simulations of Saharan dust sources, *J. Geophys. Res.*, 102, 4387–4404, 1997.

Mateos, D., Bilbao, J., Kudish, A. I., Parisi, A. V., Carbajal, G., di Sarra, A., Román, R., and de Miguel, A.: Validation of satellite erythemal radiation retrievals using ground-based measurements in five countries, *Remote Sens. Environ.*, 128, 1–10, 2013.

25 Meloni, D., di Sarra, A., Fiocco, G., and Junkermann, W.: Tropospheric aerosols in the Mediterranean: III. Measurements and modeling of actinic radiation profiles, *J. Geophys. Res.*, 108, 4323, doi:10.1029/2002JD003293, 2003.

30 Meloni, D., di Sarra, A., Herman, J. R., Monteleone, F., and Piacentino, S.: Comparison of ground-based and TOMS erythemal UV doses at the island of Lampedusa in the period 1998–2003: role of tropospheric aerosols, *J. Geophys. Res.*, 110, D01202, doi:10.1029/2004JD005283, 2005.

**Saharan dust aerosol
over the central
Mediterranean Sea**

M. Marconi et al.

Title Page

Abstract

Introduction

Conclusions

References

Tables

Figures

◀

▶

◀

▶

Back

Close

Full Screen / Esc

Printer-friendly Version

Interactive Discussion



Meloni, D., di Sarra, A., Pace, G., and Monteleone, F.: Aerosol optical properties at Lampedusa (Central Mediterranean). 2. Determination of single scattering albedo at two wavelengths for different aerosol types, *Atmos. Chem. Phys.*, 6, 715–727, doi:10.5194/acp-6-715-2006, 2006.

5 Meloni, D., di Sarra, A., Biavati, G., De Luisi, J. J., Monteleone, F., Pace, G., Piacentino, S., and Sferlazzo, D.: Seasonal behaviour of Saharan dust events at the Mediterranean island of Lampedusa in the period 1999–2005, *Atmos. Environ.*, 41, 3041–3056, 2007.

Meloni, D., di Sarra, A., Monteleone, F., Pace, G., Piacentino, S., and Sferlazzo, D. M.: Seasonal transport patterns of intense Saharan dust events at the Mediterranean island of Lampedusa
10 *Atmos. Res.*, 88, 134–148, doi:10.1016/j.atmosres.2007.10.007, 2008.

Miranda, J., Cahill, T. A., and Morales, J. R.: Determination of elemental concentrations in atmospheric aerosols in Mexico City using proton induced X-Ray emission, proton elastic scattering and laser absorption, *Atmos. Environ.*, 28, 2299–2306, 1994.

15 Nava, S., Becagli, S., Calzolari, G., Chiari, M., Lucarelli, F., Prati, P., Traversi, R., Udusti, R., Valli, G., and Vecchi, R.: Saharan dust impact in central Italy: an overview on three years elemental data records, *Atmos. Environ.*, 60, 444–452, 2012.

Pace, G., di Sarra, A., Meloni, D., Piacentino, S., and Chamard, P.: Aerosol optical properties at Lampedusa (Central Mediterranean). 1. Influence of transport and identification of different aerosol types, *Atmos. Chem. Phys.*, 6, 697–713, doi:10.5194/acp-6-697-2006, 2006.

20 Pederzoli, A., Mircea, M., Finardi, S., di Sarra, A., and Zanini, G.: Quantification of Saharan dust contribution to PM₁₀ concentrations over Italy in 2003–2005, *Atmos. Environ.*, 44, 4181–4190, 2010.

Perrino, C., Canepari, S., Cardarelli, E., Catrambone, M., and Sagolini, T.: Inorganic constituents of urban air pollution in the Lazio region (Central Italy), *Environ. Monit. Assess.*, 136, 69–86, 2008.

25 Pey, J., Querol, X., Alastuey, A., Forastiere, F., and Stafoggia, M.: African dust outbreaks over the Mediterranean Basin during 2001–2011: PM₁₀ concentrations, phenomenology and trends, and its relation with synoptic and mesoscale meteorology, *Atmos. Chem. Phys.*, 13, 1395–1410, doi:10.5194/acp-13-1395-2013, 2013.

30 Querol, X., Pey, J., Pandolfi, M., Alastuey, A., Cusack, M., Perez, N., Moreno, T., Viana, M., Mihalopoulos, N., Kallos, G., and Kleanthous, S.: African dust contributions to mean ambient PM₁₀ mass-levels across the Mediterranean Basin, *Atmos. Environ.*, 43, 4266–4427, 2009.

**Saharan dust aerosol
over the central
Mediterranean Sea**

M. Marconi et al.

[Title Page](#)[Abstract](#)[Introduction](#)[Conclusions](#)[References](#)[Tables](#)[Figures](#)[◀](#)[▶](#)[◀](#)[▶](#)[Back](#)[Close](#)[Full Screen / Esc](#)[Printer-friendly Version](#)[Interactive Discussion](#)

Rodríguez, S., Querol, X., Alastuey, A., Kallos, G., and Kakaliagou, O.: Saharan dust contributions to PM₁₀ and TSP levels in Southern and Eastern Spain, *Atmos. Environ.*, 35, 2433–2447, 2001.

5 Rodríguez, S., Alastuey, A., and Querol, X.: A review of methods for long term in situ characterization of aerosol dust, *Aeolian Res.*, 6, 55–74, 2012.

Wagener, T., Guieu, C., and Leblond, N.: Effects of dust deposition on iron cycle in the surface Mediterranean Sea: results from a mesocosm seeding experiment, *Biogeosciences*, 7, 3769–3781, doi:10.5194/bg-7-3769-2010, 2010.

10 Zender, C. S., Miller, R. L., and Tegen, I.: Quantifying mineral dust mass budgets: terminology, constraints, and current estimates, *Eos Trans. Amer. Geophys. Union*, 85, 48, 509–512, 2004.

Saharan dust aerosol
over the central
Mediterranean Sea

M. Marconi et al.

Table 1. Seasonal occurrence of different transport scenarios identified on the base of nssCa on PM_{10} and τ and α from optical measurements. The number of cases and the percent with respect to the total number of PM_{10} measurements are reported for each season. Four criteria (1 through 4) to detect dust presence in the column and at surface are established, while their combination is used to identify six possible scenarios (a through f) of dust transport. Surface and large surface desert dust episodes correspond to values of nssCa respectively larger than 483 and 2.483 ng m^{-3} . Episodes characterized by the dominant presence of desert dust aerosol on the atmospheric column are identified when $\tau > 0.15$ and $\alpha < 0.5$, while intense transport episodes are defined when $\tau > 0.25$ and $\alpha < 0.35$. Please note that the percentages in 1–4 refer to the number of occurrences in each season, while those in a–f refer to the number of cases in 1–4.

Periods	DJF	MAM	JJA	SON
Number and frequency of cases	133 (17.1 %)	229 (29.5 %)	271 (34.9 %)	143 (18.4 %)
1) Surface episode	37 (27.8 %)	68 (29.7 %)	46 (17 %)	42 (29.4 %)
a) Columnar episode	7 (18.9 %)	39 (57.4 %)	21 (45.6 %)	19 (45.2 %)
2) Large surface episode	23 (17.3 %)	36 (16 %)	13 (4.8 %)	24 (16.9 %)
b) Columnar episode	7 (30.4 %)	24 (66.6 %)	9 (69.2 %)	15 (62.5 %)
c) Large column episode	1 (4.3 %)	13 (36.1 %)	9 (69.2 %)	7 (29.2 %)
3) Columnar episode	8 (6 %)	66 (28.8 %)	77 (28.4 %)	30 (21 %)
d) Surface episode	8 (100 %)	49 (74.2 %)	43 (55.9 %)	29 (96 %)
4) Large columnar episode	1 (0.75 %)	33 (14.4 %)	36 (13.3 %)	10 (7 %)
e) Surface episode	1 (100 %)	23 (69.7 %)	18 (50.0 %)	8 (80 %)
f) Large surface episode	1 (100 %)	13 (39.4 %)	9 (25 %)	7 (70 %)

Title Page

Abstract

Introduction

Conclusions

References

Tables

Figures

◀

▶

◀

▶

Back

Close

Full Screen / Esc

Printer-friendly Version

Interactive Discussion



Saharan dust aerosol over the central Mediterranean Sea

M. Marconi et al.

Table 2. Median, mean, standard deviation of the mean and number of valid data for the percentage of metal solubility in samples classified as Saharan dust events and non-Saharan dust.

	Saharan dust event				Non Saharan dust events			
	Median	Mean	Std dev of the mean	N. valid data	Median	Mean	Std dev of the mean	N. valid data
Al	10.7	12.5	0.8	159	14.8	18.6	0.6	497
Fe	5.9	7.5	0.4	158	13.0	15.3	0.5	499
Ca	75.8	75.2	1.5	163	76.8	76.4	1.0	495
Mg	75.4	73.4	2.5	147	91.7	87.1	1.4	395
K	39.5	40.5	1.3	166	63.7	63.0	0.9	510
Mn	54.6	53.9	1.2	153	54.9	55.2	1.1	330
V	46.6	46.7	2.1	104	66.7	65.1	1.5	295
Ni	50.9	50.7	2.1	136	63.0	61.3	1.3	400
Cr	6.2	6.9	0.5	94	6.0	7.6	0.7	71
Cu	45.7	47.3	1.8	143	53.1	53.6	1.4	397
Pb	62.7	64.8	2.8	84	56.3	56.8	2.0	177

Title Page

Abstract

Introduction

Conclusions

References

Tables

Figures

◀

▶

◀

▶

Back

Close

Full Screen / Esc

Printer-friendly Version

Interactive Discussion



**Saharan dust aerosol
over the central
Mediterranean Sea**

M. Marconi et al.

[Title Page](#)[Abstract](#)[Introduction](#)[Conclusions](#)[References](#)[Tables](#)[Figures](#)[◀](#)[▶](#)[◀](#)[▶](#)[Back](#)[Close](#)[Full Screen / Esc](#)[Printer-friendly Version](#)[Interactive Discussion](#)

Table 3. Aerosol size distributions and lognormal parameterization. D_v is the diameter characteristic of the mode, and σ is the standard deviation related to the lognormal curve. V (%) and N (%) are the percentage of particles belonging to the mode expressed as particle volume and number respectively.

	D_v (μm)	σ	V (%)	N (%)
Mode 1	0.29	1.35	25.6	99.8
Mode 2	2.23	2.02	49.1	1.23×10^{-1}
Mode 3	7.18	1.77	25.3	1.89×10^{-5}

Saharan dust aerosol over the central Mediterranean Sea

M. Marconi et al.

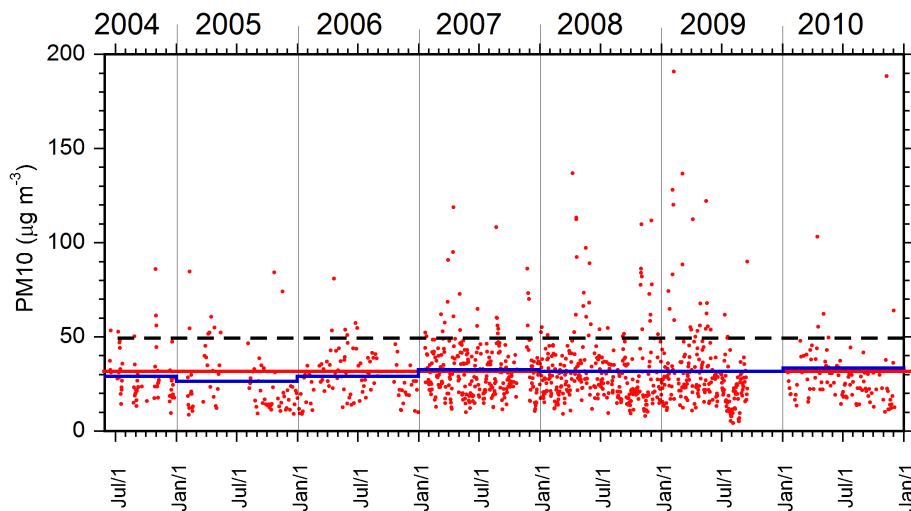


Fig. 1. Temporal evolution of PM_{10} at Lampedusa in the period June 2004–December 2010. The black dashed line represents the EU daily threshold value of $50 \mu\text{g m}^{-3}$. The red line is the mean PM_{10} over the whole sampling period and the blue one represents the annual means.

[Title Page](#)[Abstract](#)[Introduction](#)[Conclusions](#)[References](#)[Tables](#)[Figures](#)[◀](#)[▶](#)[◀](#)[▶](#)[Back](#)[Close](#)[Full Screen / Esc](#)[Printer-friendly Version](#)[Interactive Discussion](#)

Saharan dust aerosol over the central Mediterranean Sea

M. Marconi et al.

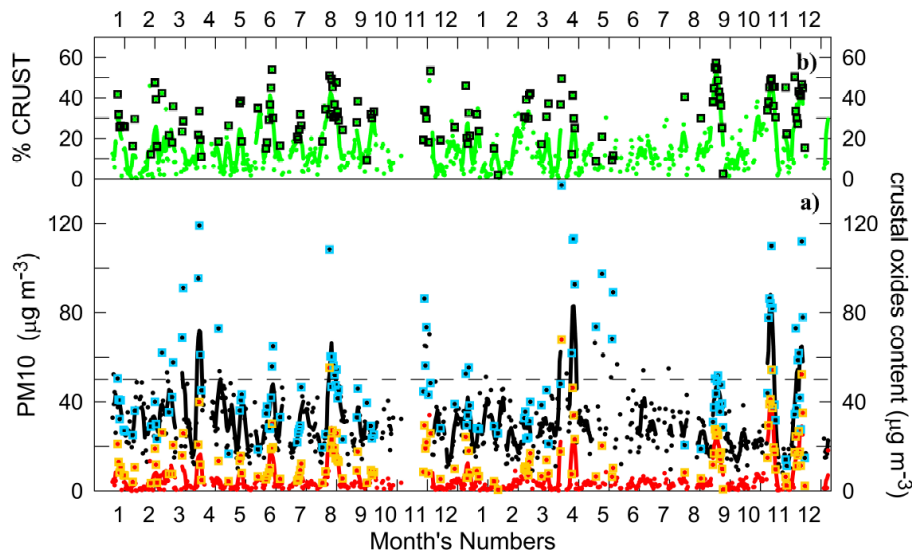


Fig. 2. (a) Temporal evolution of the PM_{10} mass concentration and of the crustal oxide content for the period January 2007 to December 2008. Daily measurements and 5-day running means are plotted respectively as black (red) dots and lines for PM_{10} (crustal content). Measurements having $nssCa > 483 \text{ ng m}^{-3}$ are evidenced by cyan and yellow open square for PM_{10} and crustal oxide content. (b) Temporal evolution of the mass ratio between crustal oxide content and PM_{10} for the period January 2007 to December 2008. Daily measurements and 5-day running means are plotted respectively as green dots and lines. Measurements having $nssCa > 483 \text{ ng m}^{-3}$ are evidenced by black open squares.

[Title Page](#)
[Abstract](#)
[Introduction](#)
[Conclusions](#)
[References](#)
[Tables](#)
[Figures](#)
[Back](#)
[Close](#)
[Full Screen / Esc](#)
[Printer-friendly Version](#)
[Interactive Discussion](#)

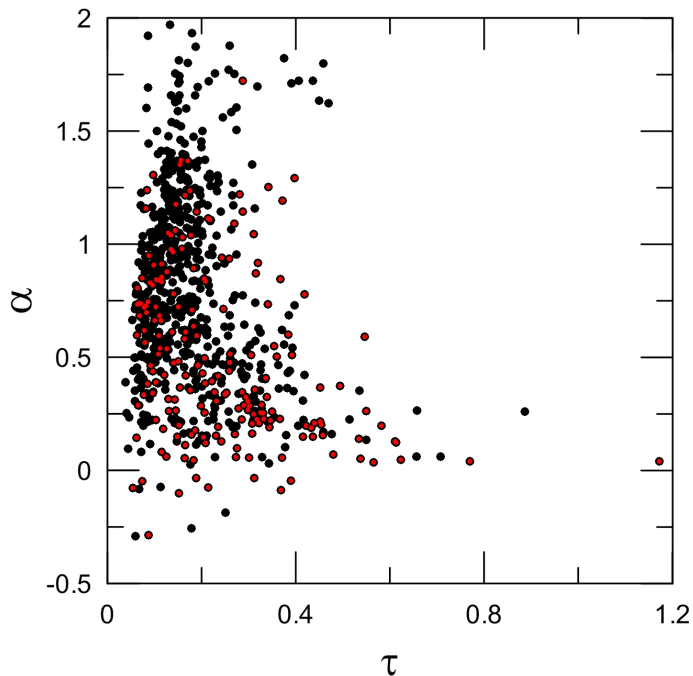


Fig. 3. Averages of aerosol Ångström exponent vs. aerosol optical depth at 495.7 nm during the period June 2004–September 2010 for the days with PM_{10} ion analyses and for cloud-free periods, when aerosol optical depth measurements are possible. The red dots represent days with $\text{nssCa} > 483 \text{ ng m}^{-3}$ (i.e. elevated dust at the surface).

Saharan dust aerosol over the central Mediterranean Sea

M. Marconi et al.

Title Page

Abstract

Introduction

Conclusions

References

Tables

Figures

◀

▶

◀

▶

Back

Close

Full Screen / Esc

Printer-friendly Version

Interactive Discussion



Saharan dust aerosol
over the central
Mediterranean Sea

M. Marconi et al.

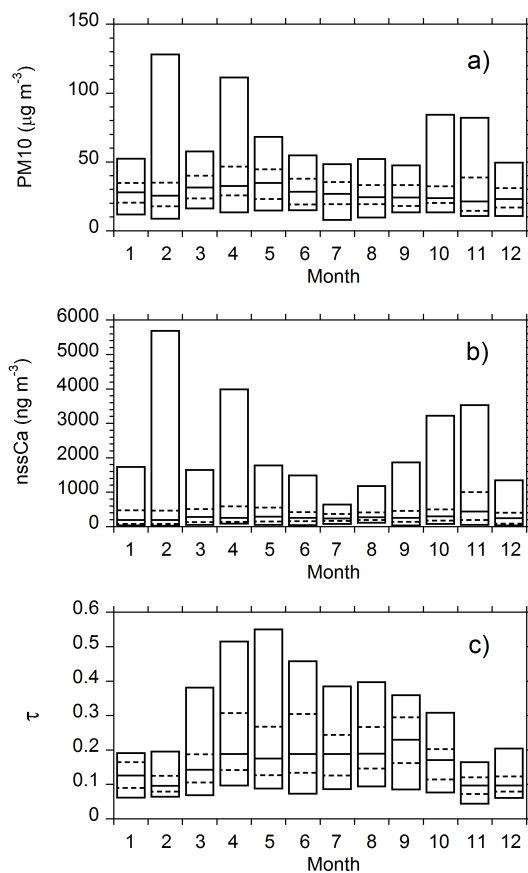


Fig. 4. Monthly distribution of PM₁₀ (a), nssCa (b), and τ (c) for the period June 2004–December 2010. The top and bottom of each box show the 5th and 95th percentiles. The middle line shows the median value, and the dashed lines show the 25th and 75th percentiles.

[Title Page](#)[Abstract](#)[Introduction](#)[Conclusions](#)[References](#)[Tables](#)[Figures](#)[◀](#)[▶](#)[◀](#)[▶](#)[Back](#)[Close](#)[Full Screen / Esc](#)[Printer-friendly Version](#)[Interactive Discussion](#)

Saharan dust aerosol
over the central
Mediterranean Sea

M. Marconi et al.

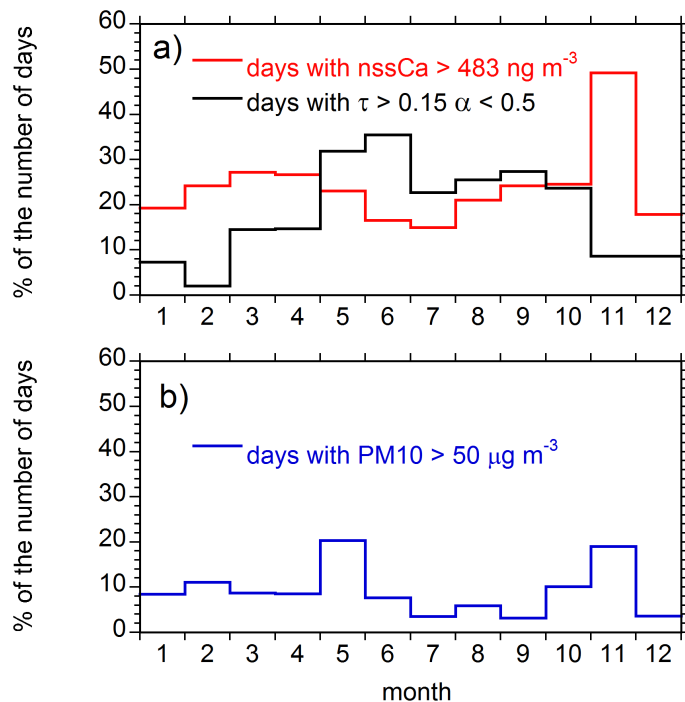


Fig. 5. (a) Percentage of Saharan dust events observed in each month identified from the aerosol optical properties (black line) and from the nssCa amount (red line) and (b) percent number of days with PM₁₀ > 50 $\mu\text{g m}^{-3}$.

Saharan dust aerosol
over the central
Mediterranean Sea

M. Marconi et al.

Title Page

Abstract

Introduction

Conclusions

References

Tables

Figures



Back

Close

Full Screen / Esc

Printer-friendly Version

Interactive Discussion

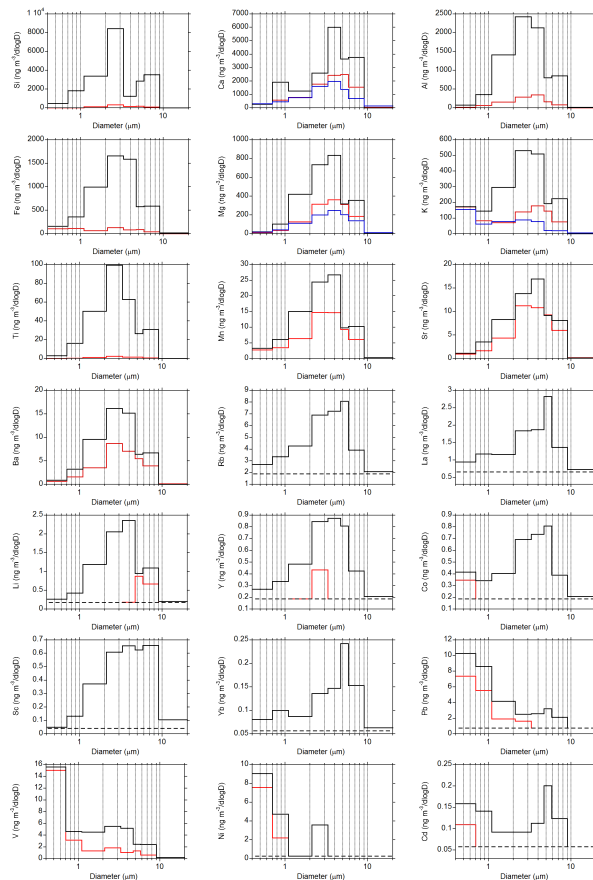


Fig. 6. Size distributions of main and trace elements during a Saharan dust event (23–26 June 2006) by using different solubilization methods: $\text{HNO}_3\text{-H}_2\text{O}_2$ in microwave oven (black line), HNO_3 in ultrasonic bath (red line), and Milli-Q water in ultrasonic bath (blue line). The dashed lines represent the instrumental detection limit for each element.

Saharan dust aerosol
over the central
Mediterranean Sea

M. Marconi et al.

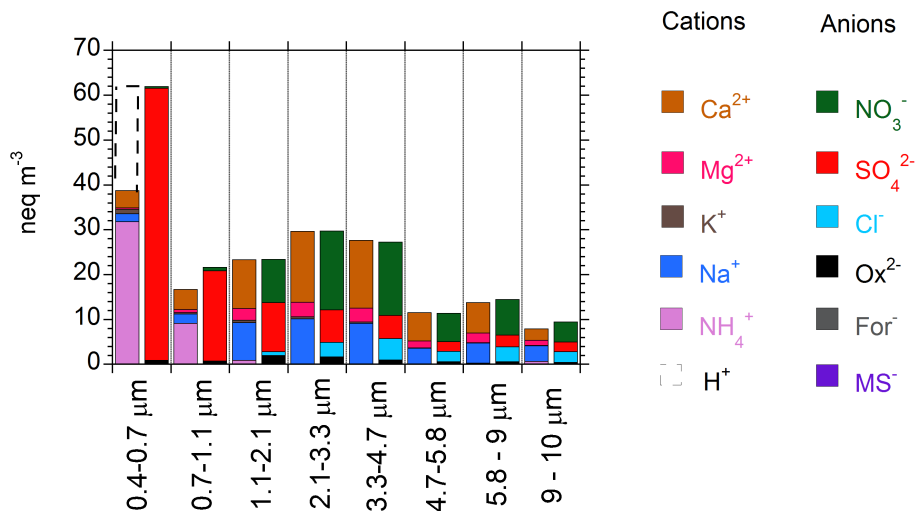


Fig. 7. Ionic balance in each of the 7 stages of the multi-stage impactor for the sampling of 23–26 June 2006, characterized by a high crustal content.

Saharan dust aerosol
over the central
Mediterranean Sea

M. Marconi et al.

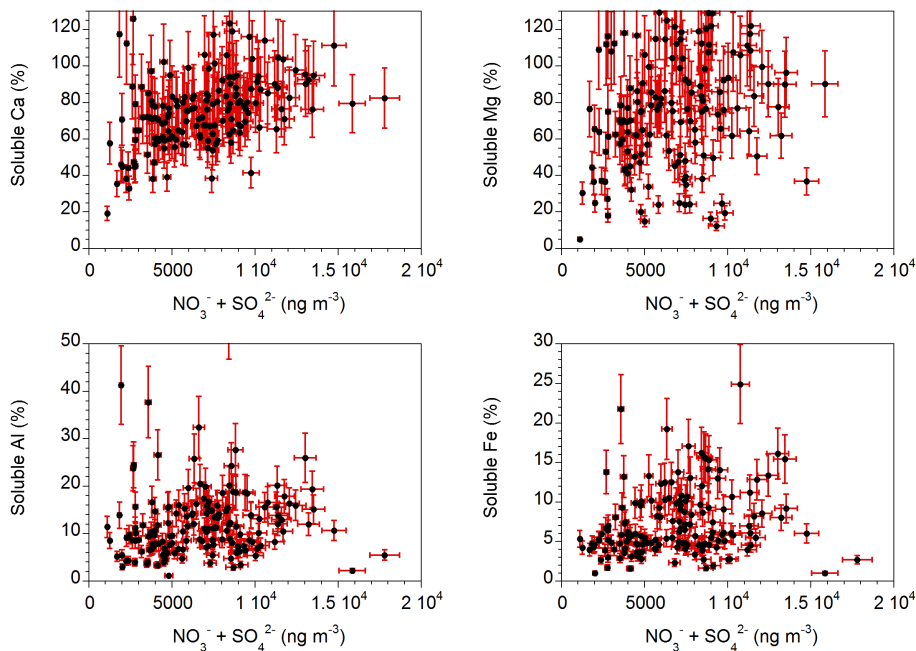


Fig. 8. Scatter plot of solubility in HNO_3 pH 1.5, calculated with respect to the total elemental content determined by PIXE, for Ca, Mg, Al and Fe as a function of the sum of nitrate and sulfate for days characterized by high crustal content ($\text{nssCa} > 483 \text{ ng m}^{-3}$).

Title Page

Abstract

Introduction

Conclusions

References

Tables

Figures

◀

▶

◀

▶

Back

Close

Full Screen / Esc

Printer-friendly Version

Interactive Discussion

